Research Square

Preprints are preliminary reports that have not undergone peer review.
They should not be considered conclusive, used to inform clinical practice,
or referenced by the media as validated information.

Geochemical behavior and dietary exposure risks of rare earth elements in a soil-rice system from a typical karst catchment, Southwest China

Qi Liu
Huazhong Agricultural University
Sheng Wang
Chuxiong Normal University
Tao He
Chinese Academy of Sciences
Jijiang Zhou
Jilin Agricultural University
Xuchao Sun
Huazhong Agricultural University
Li Bao
Yunnan Agricultural University
Wenbing Zhou
Huazhong Agricultural University
Naiming Zhang
zhangnaiming@sina.com

Yunnan Agricultural University

Research Article

Keywords: Rare earth elements, Karst, Soil-rice system, Health risk assessment, Geogenic enrichment

Posted Date: June 8th, 2026

DOI: https://doi.org/10.21203/rs.3.rs-9787387/v1

License: This work is licensed under a Creative Commons Attribution 4.0 International License.
Read Full License

Additional Declarations: No competing interests reported.

Version of Record: A version of this preprint was published at Journal of Soils and Sediments on October 5th, 2026. See the published version at https://doi.org/10.1007/s11368-026-04579-0.

Geochemical behavior and dietary exposure risks of rare earth elements in a soil-rice system from a typical karst catchment, Southwest China

Qi Liu [1,3], Sheng Wang [3,4], Tao He [5], Jijiang Zhou [6], Xuchao Sun [1], Li Bao [2,3], Wenbing Zhou [1,*], Naiming Zhang [2,3,*]

[1] College of Resources and Environment, Huazhong Agricultural University, Wuhan 430070, China

[2] College of Resources and Environment, Yunnan Agricultural University, Kunming 650201, China

[3] Yunnan Soil Fertilizer and Pollution Repair Engineering Research Center, Kunming 650201, China

[4] School of Chemistry and Geographical Sciences, Chuxiong Normal University, Chuxiong 675000, Yunnan, China

[5] Kunming Institute of Botany, Chinese Academy of Sciences, Kunming 650201, China

[6] College of Mycology, Jilin Agricultural University, Changchun 130118, China

Qi Liu: liuqi6766@163.com

Sheng Wang: wangshengynu@163.com

Tao He: hetao1@mail.kib.ac.cn

Jijiang Zhou: 18843183341@163.com

Xuchao Sun: xuchao.sun@webmail.hzau.edu.cn

Li Bao: bbllty@163.com

* Corresponding author

Wenbing Zhou: zhouwb@mail.hzau.edu.cn; +86 13545387980 (Tel).

Naiming Zhang: zhangnaiming@sina.com; +86 13308803918 (Tel).

Abstract

Purpose

Karst landscapes in Southwest China are characterized by significant geogenic enrichment of rare earth elements (REEs); however, the geochemical behavior and dietary exposure risks within the soil-rice system in Yunnan Province remain insufficiently understood. This study aimed to characterize the distribution of REEs, elucidate their fractionation mechanisms along the soil-plant continuum, and quantitatively evaluate the potential health risks for local residents in a typical karst agricultural catchment.

Methods

Paired samples of paddy soils and rice tissues (roots, stems and leaves, and grains) were collected from a karst area developed on the Triassic Gejiu Formation in Qiubei County, Yunnan, with sandstone-derived soils serving as regional controls. Concentrations of 14 REEs were determined using ICP-MS. Geochemical parameters, including NASC-normalized patterns, cerium (δCe) and europium (δEu) anomalies, and bio-concentration factors (BCF), were employed to trace the soil-to-grain transfer. Human health risks were assessed using the target hazard quotient (THQ) and hazard index (HI) approaches.

Results

Karst soils exhibited significantly elevated total REE concentrations ($\sum$REE = 287.6 ± 48.3 $mg \cdot kg^{-1}$), which were 1.6 times higher than the provincial background. These soils inherited distinct negative Ce (0.76 ± 0.08) and Eu (0.65 ± 0.05) anomalies from the underlying limestone bedrock, providing a robust lithogenic fingerprint. Within rice plants, $\sum$REE decreased by two orders of magnitude from roots (1284.6 $\mu g \cdot kg^{-1}$) to grains (31.5 $\mu g \cdot kg^{-1}$), with a mean root bio-concentration factor (BCF_{root}) of 0.0045. Along the translocation pathway, the Ce anomaly was attenuated (from 0.76 to 0.89) and the light to heavy rare earth element ratios (*LREE/HREE*) decreased, reflecting preferential HREE mobility and rhizosphere-mediated Ce redox shifts. The cumulative HI for adults was 0.158, well below the safety threshold of 1.0.

Conclusion

Despite the geogenic enrichment of REEs in karst soils, robust physiological barriers in rice plants effectively restrict their translocation to edible tissues. The study confirms that rice produced in the Yunnan karst region is safe for consumption, with health risks remaining well below safety thresholds. These results support the sustainable agricultural use of high-background carbonate terrains and provide a scientific framework for regional food safety management.

Keywords: Rare earth elements; Karst; Soil-rice system; Health risk assessment; Geogenic enrichment

1 Introduction

Rare earth elements (REEs) comprise the 14 elements of the lanthanide series from lanthanum (La) to lutetium (Lu). Based on their ionic radii, they are typically categorized into three subgroups: light (LREE; La–Sm), middle (MREE; Eu–Ho), and heavy (HREE; Er–Lu) REEs (Mori et al. 2025). China holds a preeminent global position in REE resources, possessing the largest reserves, production, and export volumes (Xu et al. 2025b). While REEs are indispensable for high-tech industries and are utilized as micro-fertilizers in agriculture (Ribeiro et al. 2024), their extensive extraction and industrial application release these elements into atmospheric dust and water systems, facilitating their bioaccumulation in the food chain (Yang et al. 2022; Yun et al. 2024). As non-essential elements for biological development, excessive REE exposure poses significant risks to human health. Chronic intake, even at minimal levels, has been linked to neurotoxicity, reproductive system impairment, metabolic disorders, and potentially carcinogenic effects (Zhang et al. 2014; Pagano et al. 2015). Consequently, REEs are increasingly classified as a novel class of emerging environmental contaminants (Wang et al. 2024). Beyond their ecotoxicological implications, REEs serve as sensitive geochemical tracers in the Earth's critical zone; their coherent yet predictable fractionation patterns provide deep insights into rock weathering, soil formation, and elemental cycling (Laveuf and Cornu 2009; Li et al. 2025b).

Karst environments are unique and intricate landscapes that cover approximately 15% of the Earth's total land area, with major distributions along the European Mediterranean coast, the Caribbean, and the Yunnan-Guizhou Plateau in China (Jiang et al. 2014; Hartmann et al. 2014). These environments are primarily formed by the dissolution of soluble carbonate rocks and are characterized by a distinct dualistic structure comprising surface bedrock/soil and subsurface caves and underground rivers (Gutiérrez et al. 2014; Veress 2020). Karst ecosystems are highly sensitive to ecological changes and possess a limited tolerance for environmental disturbances (Shi et al. 2019; Liu et al. 2022). In Southwest China, the preferential leaching of calcium and magnesium during intense carbonate weathering leads to the relative enrichment of immobile REEs in residual terra rossa soils (Liu et al. 2025). Consequently, REE concentrations in these karst soils often significantly exceed national background values. Furthermore, karst regions face severe challenges from soil erosion and rock desertification, which modify soil hydrological processes and elemental transport mechanisms (Cao et al. 2021; Xu et al. 2025a). While REE geochemistry has been extensively studied in the karst regions of Guizhou and Guangxi (Xiong et al. 2021; Dong et al. 2024), Yunnan Province—a critical transition zone with a unique plateau subtropical monsoon climate and specific lithological units such as the Triassic Gejiu Formation—has received limited research attention (Sun et al. 2023; Shi et al. 2025).

Rice (*Oryza sativa* L.) is one of the most important global food crops, serving as the primary staple for more than half of the world's population (Zaghum et al. 2022; Wang et al. 2025). In Yunnan Province, rice is the predominant staple crop, and its cultivation in karst soils with high geogenic REE backgrounds represents a critical pathway for human exposure (Cai et al. 2025; Xu et al. 2026). Previous research in

other karst areas suggests that despite high total REE concentrations in soil, their bioavailability may be limited by specific physicochemical properties (Zhang et al. 2019; Han and Xu 2021). However, the specific "soil-to-grain" transfer efficiency and the internal physiological barrier mechanisms within rice plants under the unique geochemical conditions of the Yunnan plateau remain poorly understood. Furthermore, there is a lack of quantitative evidence to address whether the geogenic enrichment of REEs in these agricultural soils translates into a genuine non-carcinogenic health risk for local residents (Hao et al. 2026).

To bridge these knowledge gaps, this study focuses on a typical karst agricultural catchment in Qiubei County, Yunnan Province. Our specific objectives are: (1) to determine the distribution and NASC-normalized patterns of REEs in the soil-rice system; (2) to elucidate the fractionation mechanisms of REEs during their translocation from soil to various rice organs, with a focus on Ce and Eu anomalies; and (3) to quantitatively assess the non-carcinogenic health risks associated with rice consumption using the target hazard quotient (THQ) approach (Ain et al. 2023).

2 Materials and Methods

2.1 Study Area and Sampling

The study area is situated in Qiubei County, Wenshan Prefecture, southeastern Yunnan Province, China (24°02′–24°08′ N, 104°04′–104°12′ E). This region features a representative peak-cluster depression karst landscape developed on the Middle Triassic Gejiu Formation (T_2g) limestones. The closed micro-catchment structure of karst depressions facilitates the accumulation of weathered materials and sediments from surrounding slopes, providing an ideal setting for investigating soil-plant elemental cycling. The climate is classified as a subtropical plateau monsoon, with a mean annual temperature of 16.3 °C and mean annual precipitation of 1,174 mm. Agricultural activities in the depressions are dominated by paddy fields with a cultivation history exceeding 50 years, primarily irrigated by natural precipitation and local karst springs (Sun et al. 2023).

In September 2024, during the rice harvest season, 30 paired soil-rice plant samples were collected from the karst paddy fields. For regional comparison, 15 soil samples were obtained from non-karst (sandstone-derived) agricultural fields approximately 20 km away to serve as controls. At each site, rhizosphere soil (0–20 cm depth) was collected using a stainless steel auger following standard protocols. Corresponding rice plants were carefully uprooted, rinsed thoroughly with deionized water to remove adhering soil particles, and partitioned into three components: roots, stems and leaves, and grains (brown rice). All samples were sealed in polyethylene bags, transported to the laboratory in an ice-cooled container, and stored at 4 °C prior to further processing.

2.2 Sample Preparation and Chemical Analysis

Soil samples were air-dried at room temperature, homogenized using an agate mortar, and passed through a 200-mesh (74 μm) nylon sieve. Soil pH was determined in a 1:2.5 (m/v) soil-to-water suspension using a digital pH meter. Soil organic matter was quantified via the potassium dichromate oxidation-titration method, and cation exchange capacity (CEC) was measured using the ammonium acetate exchange method at pH 7.0.

For total REE determination, approximately 50 mg of soil powder was digested in a high-pressure Teflon bomb with a concentrated HF-HNO_3 (1:1, v/v) mixture at 190 °C for 48 h. Plant tissues (roots, stems and leaves, and grains) were oven-dried at 70 °C to a constant weight, pulverized, and a 200 mg aliquot was digested with a concentrated HNO_3-H_2O_2 mixture using a microwave-assisted system.

The concentrations of 14 REEs (La, Ce, Pr, Nd, Sm, Eu, Gd, Tb, Dy, Ho, Er, Tm, Yb, Lu) were analyzed by inductively coupled plasma mass spectrometry (ICP-MS, Agilent 7900). To ensure analytical precision and compensate for matrix effects, Indium (In) and Rhenium (Re) were employed as internal standards. Quality assurance and quality control (QA/QC) were maintained through the analysis of procedural blanks and certified reference materials (CRMs), including GBW07403 for soil and GBW10015 for plant tissues. The recovery rates for all target elements were within the range of 92% to 108%.

2.3 Data Processing and Geochemical Parameters

To facilitate the identification of geochemical fractionation patterns, REE concentrations in all samples were normalized against the North American Shale Composite (NASC) values (Gromet et al. 1984). The total REE content (∑REE) was defined as the sum of the 14 analyzed elements. The fractionation between light REEs (LREEs, La to Eu) and heavy REEs (HREEs, Gd to Lu) was evaluated using the *LREE/HREE* ratio based on normalized values. To quantify the enrichment or depletion of specific elements relative to their neighbors, cerium (δCe) and europium (δEu) anomalies were calculated using the following geometric mean equations:

$$\delta\mathrm{Ce} = \frac{\mathrm{Ce}_N}{(\mathrm{La}_N \times \mathrm{Pr}_N)^{0.5}} \quad (1)$$

$$\delta\mathrm{Eu} = \frac{\mathrm{Eu}_N}{(\mathrm{Sm}_N \times \mathrm{Gd}_N)^{0.5}} \quad (2)$$

where the subscript N denotes NASC-normalized concentrations. In this study, δ values greater than 1.05 or less than 0.95 were considered to indicate significant positive or negative anomalies, respectively (Barrat et al. 2023).

The mobility and accumulation of REEs within the soil-rice system were quantified using the bio-concentration factor (BCF_{root}) and translocation factors (TF):

$$BCF_{root} = \frac{C_{root}}{C_{Soil}} \quad (3)$$

$$TF_{stem/root} = \frac{C_{stem}}{C_{root}} \quad (4)$$

$$TF_{grain/stem} = \frac{C_{grain}}{C_{stem}} \quad (5)$$

where C_{Soil}, C_{root}, C_{stem}, and C_{grain} represent the REE concentrations in the rhizosphere soil, roots, stems and leaves, and grains, respectively.

2.4 Health Risk Assessment

The potential non-carcinogenic health risks for local residents through rice consumption were evaluated using the Target Hazard Quotient (THQ) method as established by the U.S. Environmental Protection Agency (1989). This approach incorporates parameters such as the estimated daily intake (EDI), oral reference dose (RfD), and average body weight. To quantify the exposure level, the EDI (μg $\cdot kg^{-1}$ body weight/day) for each REE was calculated as follows:

$$EDI = \frac{(C \times IR \times EF \times ED)}{(BW \times AT)} \quad (6)$$

Where C represents the REE concentration in rice grains ($\mu g \cdot kg^{-1}$), while IR denotes the daily ingestion rate of rice, set at 300 g/day for adults in the study region. The exposure frequency (EF) and duration (ED) were defined as 365 days/year and 70 years, respectively. The average body weight (BW) was assumed to be 60 kg, and the averaging time (AT) was calculated as the product of ED and 365 days/year. The THQ for each element was then derived as:

$$THQ = \frac{EDI}{RfD} \quad (7)$$

where RfD is the oral reference dose. Given the absence of a unified RfD for all REEs in international guidelines, a conservative value of 1.0 $\mu g \cdot kg^{-1} \cdot bw^{-1} \cdot day^{-1}$ was adopted for each element. To account for the cumulative effect of the 14 analyzed REEs, the Hazard Index (HI) was calculated as the sum of the individual THQ values ($HI = \sum THQ$). According to the established risk characterization criteria, an HI value below 1.0 indicates that the non-carcinogenic health risk to the local population is negligible (Aarab et al. 2026).

2.5 Statistical Analysis

Statistical analyses were performed using the SPSS 31.0 software package. Prior to parametric testing, the normality of the data distribution was assessed using the Shapiro-Wilk test. To evaluate the significant differences in REE concentrations and soil physicochemical properties between the karst and control groups, a one-way analysis of variance (ANOVA) was conducted, followed by Tukey's post-hoc test for multiple comparisons. Furthermore, Pearson correlation analysis was employed to explore the relationships between soil properties and REE transfer parameters. For all statistical evaluations, a significance level of $p < 0.05$ was adopted to denote statistical significance. Data visualization and the generation of geochemical plots, including the correlation heatmap, were carried out using OriginPro 2025 software.

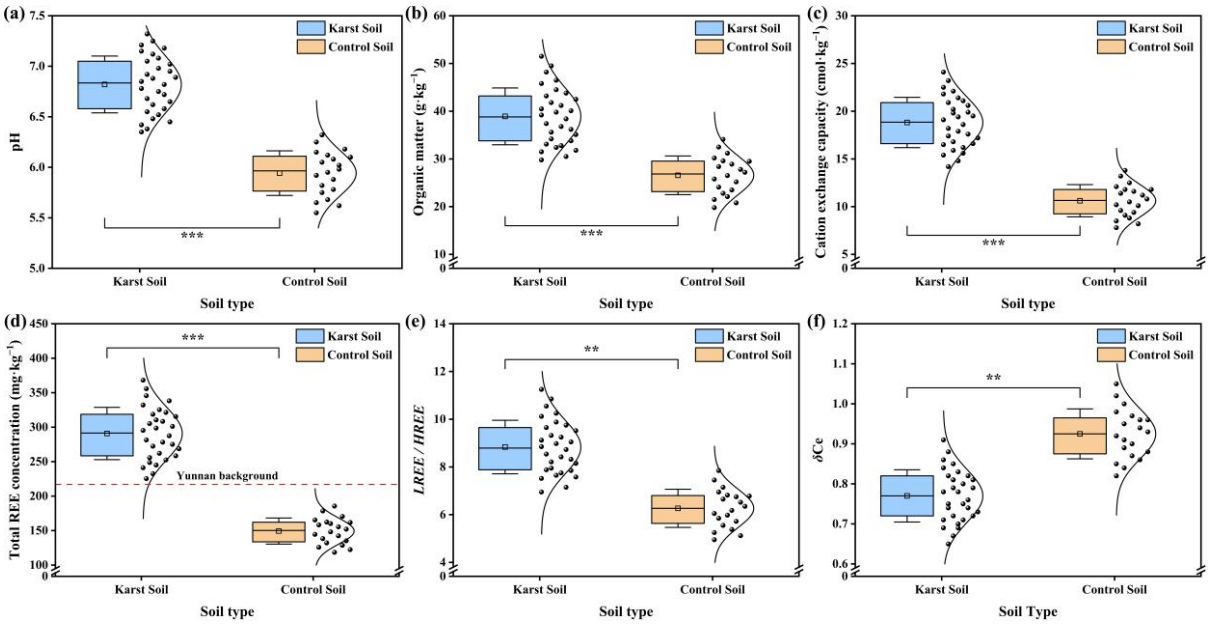
3 Results

3.1 Soil Physicochemical Properties and REE Concentrations

The physicochemical properties of the studied soils exhibited distinct contrasts between the karst and control areas (Fig. 1a-c). Karst soils were characterized by a shift toward neutrality, with pH values significantly higher than those of the acidic control soils (Fig. 1a). Notably, the nutrient buffering capacity of karst soils was substantially greater, as evidenced by organic matter (Fig. 1b) and CEC (Fig. 1c) levels that were approximately 47% and 79% higher than the control group, respectively ($p < 0.001$). These results indicate that the karst pedogenic process on the Gejiu Formation promotes the accumulation of organic components and enhances the soil's ion-retention capacity.

Regarding REE accumulation, karst soils showed a significant geogenic enrichment. The mean ∑REE in karst soils was approximately 1.96 times that of the control soils and exceeded the Yunnan provincial background by 32.6% (Fig. 1d). As illustrated in Fig. 1d, the karst area not only exhibited higher median concentrations but also a much broader range of ∑REE, reflecting the geochemical heterogeneity inherent in carbonate weathering.

The fractionation parameters further distinguished the two soil types. Karst soils were more heavily enriched in light REEs (LREEs) relative to heavy REEs (HREEs), with an *LREE/HREE* ratio approximately 1.4 times that of the control soils (Fig. 1e). Furthermore, both soil types inherited negative Ce and Eu anomalies (Fig. 1f, g), but these deficits were significantly more pronounced in the karst terrain. Specifically, the Ce deficit (δCe) in karst soils was 16% more severe than in control soils, providing a distinct lithogenic signature of the underlying limestone bedrock.



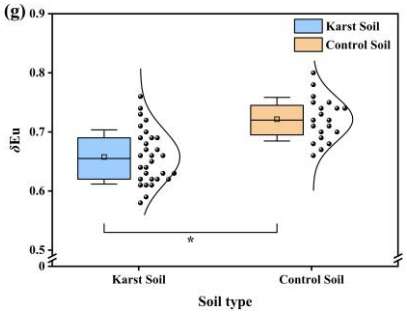


Fig. 1. Comparison of soil physicochemical properties and rare earth element (REE) characteristics between karst and control soils.

Note: (a) pH; (b) Organic matter; (c) Cation exchange capacity (CEC); (d) Total REE concentration (∑REE); (e) The ratio of light to heavy REEs (*LREE/HREE*); (f) Cerium anomaly (δCe); (g) Europium anomaly (δEu). The boxes represent the interquartile range (25th–75th percentiles); the square within the box represents the mean, and the horizontal line indicates the median. The whiskers extend to the minimum and maximum values. Individual data points are plotted to the right of each box to show the distribution, with a normal distribution curve overlaid on each group to visualize data density. In panel (d), the red dashed line denotes the Yunnan provincial soil background value (216.97 mg kg^{-1}), which is calculated as the sum of 14 individual REEs (China National Environmental Monitoring Centre 1990). Asterisks denote significant differences between karst and control soils (* $p < 0.05$, ** $p < 0.01$, *** $p < 0.001$).

3.2 The REE Distribution Patterns and Anomalies in Soils

The NASC-normalized REE patterns revealed a distinct divergence in fractionation between the two soil types (Fig. 2). Karst soils exhibited a consistent LREE-enriched configuration, with normalized LREE concentrations (La–Sm) exceeding 1.5, while HREEs (Gd–Lu) remained below unity (< 1.0). In contrast, the control soils displayed a relatively flat distribution, with normalized values hovering near the NASC reference line.

A defining geochemical feature of the karst soils was the presence of pronounced negative anomalies. The Ce anomaly (δCe) in karst soils averaged 0.76 ± 0.08, manifesting as a sharp "V-shaped" trough in the distribution curve. This deficit was significantly more severe than the minor Ce depletion observed in control soils (δCe = 0.91 ± 0.06). Similarly, the Eu anomaly (δEu) in karst soils was notably lower (0.65 ± 0.05) than in the control group. Crucially, the REE distribution pattern of the karst soils closely mirrored the geochemical signature of the underlying Triassic limestone bedrock (Fig. 2). This high degree of correspondence indicates that both the LREE-enriched trend and the characteristic Ce depletion are robustly inherited from the parent carbonate lithology during pedogenesis.

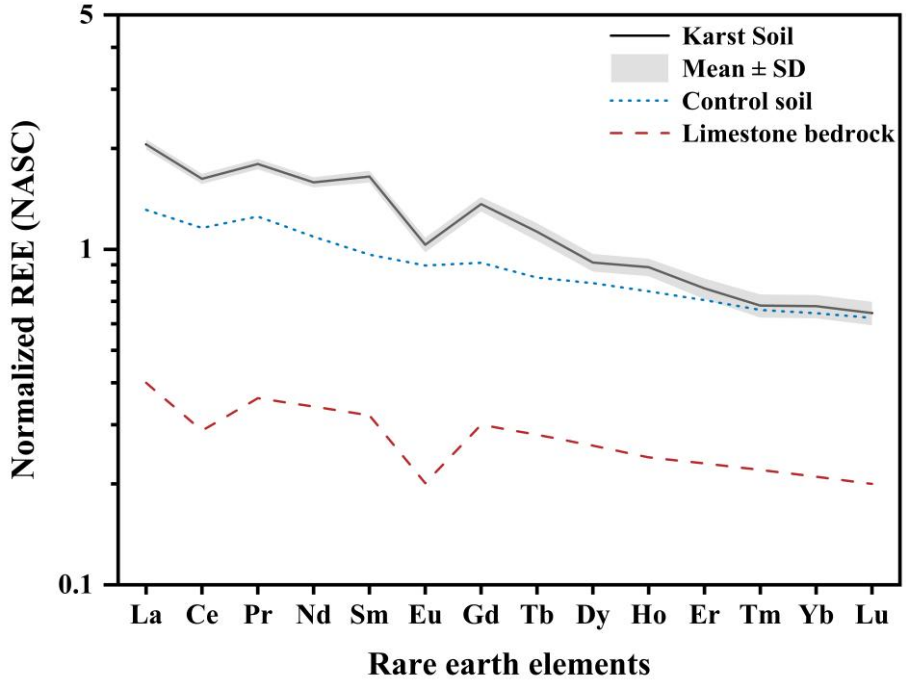


Fig. 2. NASC-normalized rare earth element (REE) distribution patterns.

Note: The black solid line and gray shaded area represent the mean and standard deviation (SD) of karst soils. The blue dotted line represents control soils, and the red dashed line represents the limestone bedrock. The Y-axis is presented on a logarithmic scale (Log_{10}). NASC: North American Shale Composite.

3.3 The REE Distribution in Rice Tissues

The distribution of REEs within the rice plant followed a steep acropetal gradient, characterized by a systematic decrease in concentrations from the underground to the aerial organs (Fig. 3a). Roots served as the primary reservoir, sequestering over 80% of the total REE burden absorbed by the plant. The ∑REE concentrations in the roots were approximately 4.5-fold higher than those in the stems and leaves, and nearly 40-fold higher than in the grains. This two-order-of-magnitude reduction, as visualized on the logarithmic scale in Fig. 3a, underscores the presence of robust physiological barriers that restrict the upward translocation of REEs, particularly into the reproductive tissues.

Internal REE fractionation also evolved significantly along the transport pathway. The *LREE/HREE* ratio exhibited a progressive decline from the roots (7.92) to the grains (4.56), representing a 42% decrease (Fig. 3b). This downward trend indicates that while LREEs are more effectively immobilized in the root system, HREEs possess higher mobility during xylem and phloem transport.

Furthermore, the Ce anomaly (δCe) showed a systematic "recovery" or attenuation as REEs moved toward the grain (Fig. 3c). The pronounced negative anomaly inherited by the roots (δCe = 0.81) gradually weakened, reaching a near-background value in the grains (δCe = 0.89). In contrast, the Eu anomaly (δEu) remained relatively stable across all tissues (Fig. 3d), suggesting that unlike the redox-sensitive Ce, Eu does not undergo significant preferential fractionation relative to its neighboring lanthanides during internal physiological cycling.

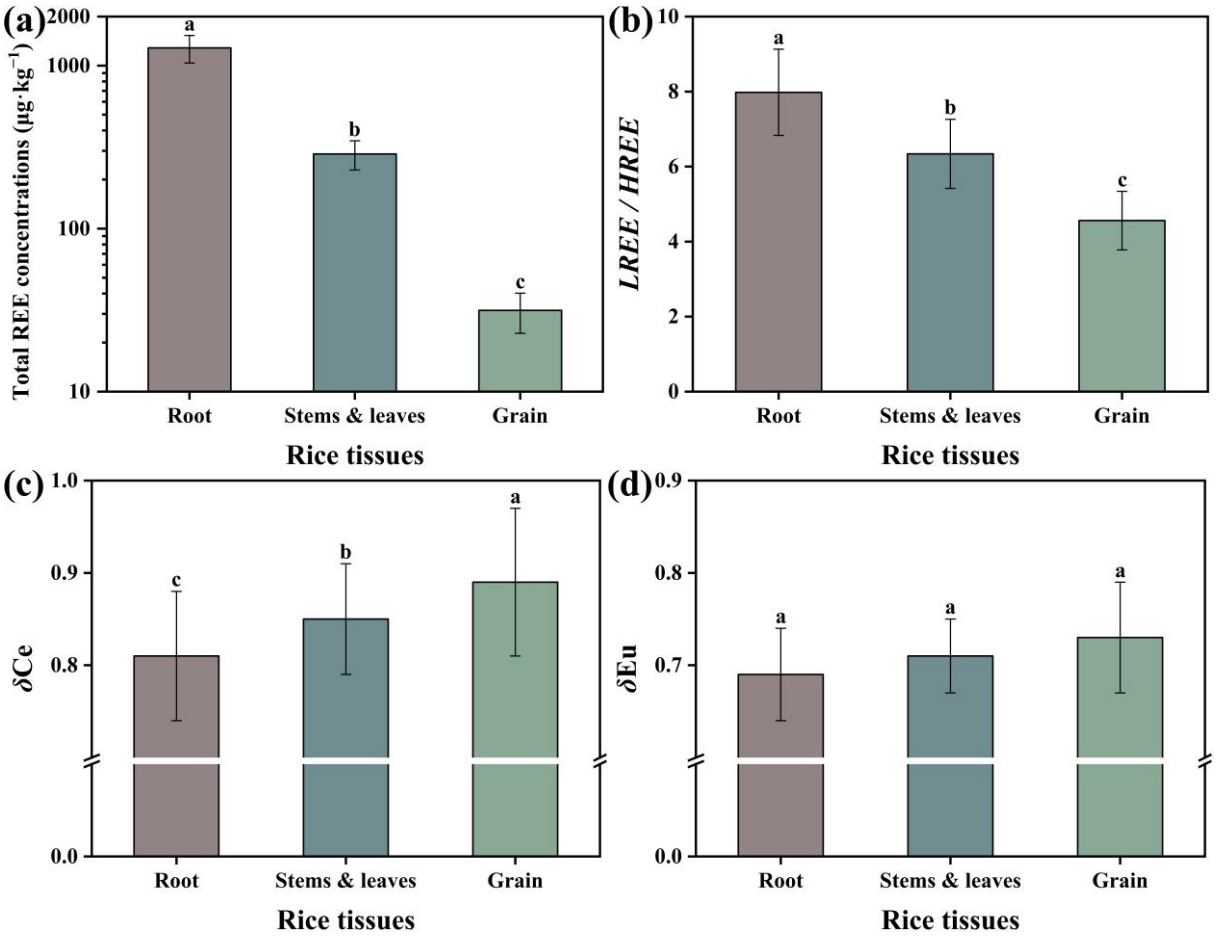


Fig. 3. Rare earth element (REE) concentrations and geochemical parameters in different rice tissues.

Note: (a) Total REE concentrations (∑REE) presented on a logarithmic scale (Log_{10}); (b) The ratio of light to heavy REEs (*LREE/HREE*); (c) Cerium anomaly (δCe); (d) Europium anomaly (δEu). Different lowercase letters (a, b, c) above the bars indicate significant differences among tissues at the $p < 0.05$ level (one-way ANOVA followed by Tukey's test). Error bars represent standard deviations. REE: rare earth element; LREE: light rare earth element; HREE: heavy rare earth element. All concentrations are reported on a dry weight (dw) basis.

3.4 Soil-Plant Transfer Factors

The migration of REEs within the soil-rice system was characterized by extremely low bioavailability and restricted internal mobility. The mean BCF_{root} (0.0045) indicates that less than 0.5% of the total REE pool in the karst rhizosphere was successfully intercepted by the root system. This minimal uptake efficiency suggests that the vast majority of geogenic REEs remain immobilized in the soil matrix, likely due to the near-neutral pH and high buffering capacity of the karst soils.

Internal translocation was subject to progressive physiological restriction at different vascular interfaces. The efficiency of REE transport from roots to stems ($TF_{stem/root}$ = 0.224) was approximately twofold higher than the transport from stems to grains ($TF_{grain/stem}$ = 0.110). This significant decrease in translocation factors suggests that the transition from vegetative tissues to reproductive organs represents a more stringent physiological bottleneck than the initial root-to-stem pathway, effectively

safeguarding the grains from REE accumulation.

Element-specific analysis revealed a clear fractionation across the lanthanide series (Fig. 4). The BCF_{root} values exhibited a monotonic increase from La (0.0038) to Lu (0.0058), with the uptake efficiency of the heaviest REE (Lu) being approximately 50% higher than that of the lightest (La). This upward trend across the atomic numbers confirms the preferential absorption of HREEs over LREEs in the karst environment, a phenomenon potentially driven by the higher stability of HREE-organic complexes in the soil solution or their smaller ionic radii, which may facilitate easier membrane transport.

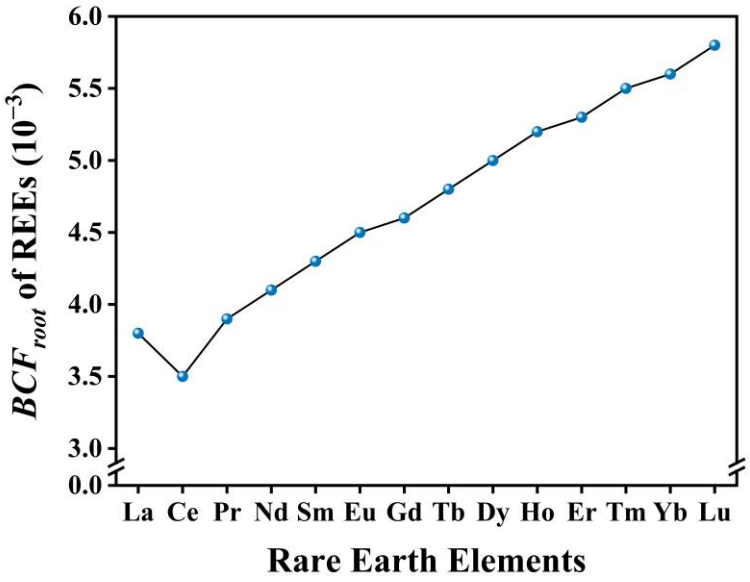


Fig. 4. Element-specific bio-concentration factors (BCF_{root}) of REEs from soil to rice roots.

Note: The data points represent the mean values. The upward trend from La to Lu illustrates the preferential accumulation of heavy REEs (HREEs) over light REEs (LREEs) in rice roots. BCF: bio-concentration factor; REE: rare earth element.

3.5 Health Risk Assessment

The dietary exposure and associated health risks from REE intake via rice consumption are summarized in Table 1. The total estimated daily intake (∑EDI) for local adults was 0.1576 $\mu g \cdot kg^{-1} \cdot bw^{-1} \cdot day^{-1}$, a value primarily driven by light REEs (LREEs). Specifically, Ce, La, and Nd were the dominant contributors, collectively accounting for over 88% of the total REE exposure. In contrast, the intake of heavy REEs (HREEs) was negligible, with elements such as Tm, Yb, and Lu contributing less than 0.1% to the total EDI.

Risk characterization revealed that the Target Hazard Quotient (THQ) for every individual REE was at least one order of magnitude below the critical safety threshold of 1.0 (Table 1). The highest individual risk was associated with Ce (THQ = 0.0718), which remained well within the safe range. Consequently, the cumulative Hazard Index (HI) for the 14 analyzed REEs was 0.158, representing only 15.8% of the maximum permissible risk level. These results provide quantitative evidence that despite

the geogenic enrichment of REEs in the karst paddy soils, the consumption of locally produced rice poses a negligible non-carcinogenic health risk to the resident population.

Table 1 Estimated daily intake (EDI) and target hazard quotient (THQ) of REEs via rice consumption for local adults.

Element	Grain concentration ($\mu g \cdot kg^{-1}$)	EDI / THQ ($\mu g \cdot kg^{-1} \cdot bw^{-1} \cdot day^{-1}$)
La	7.82 ± 2.04	0.0391
Ce	14.35 ± 4.12	0.0718
Pr	1.62 ± 0.38	0.0081
Nd	5.48 ± 1.45	0.0274
Sm	0.95 ± 0.28	0.0048
Eu	0.14 ± 0.05	0.0007
Gd	0.62 ± 0.18	0.0031
Tb	0.08 ± 0.03	0.0004
Dy	0.31 ± 0.11	0.0016
Ho	0.05 ± 0.02	0.0003
Er	0.04 ± 0.02	0.0002
Tm	0.02 ± 0.01	0.0001
Yb	0.02 ± 0.01	0.0001
Lu	0.01 ± 0.01	0.00005
∑REE	31.51 ± 8.71	/
∑EDI / HI	/	0.1576

Note: REE, EDI, THQ, and HI represent rare earth element, estimated daily intake, target hazard quotient, and hazard index, respectively. Grain concentrations are presented as mean ± standard deviation (SD). The oral reference dose (RfD) for each individual REE was set at 1.0 $\mu g \cdot kg^{-1} \cdot bw^{-1} \cdot day^{-1}$; therefore, the numerical values of EDI and THQ are identical and presented in a single column. ∑EDI represents the total estimated daily intake of all 14 REEs, and HI represents the cumulative sum of their THQ values.

3.6 Relationships between Soil Properties and REE Transfer Parameters

Pearson correlation analysis identified soil physicochemical properties as the dominant controls on REE mobility and compartmentalization (Fig. 5). The initial uptake of REEs by rice roots was governed by a strong inhibitory mechanism; soil pH, organic matter, and CEC all exhibited near-perfect negative correlations with BCF_{root} ($r < -0.97$, $p < 0.05$). These robust inverse relationships demonstrate that the near-neutrality and high nutrient buffering capacity of karst soils act as a primary geochemical filter, effectively reducing the pool of bioavailable REEs in the soil solution and suppressing their interception by the root system.

In contrast, soil properties exerted a divergent influence on the internal translocation of REEs. While organic matter restricted initial bioavailability, it showed a strong positive correlation with the

upward transport from stems to grains ($TF_{grain/stem}$, r = 0.927). This suggests a dual-function role for organic components: immobilizing REEs within the soil matrix while potentially facilitating the acropetal migration of the absorbed fraction, likely through the formation of mobile organic-REE complexes. Furthermore, the high degree of synergy observed between $TF_{stem/root}$ and $TF_{grain/stem}$ (r = 0.962) points to a coordinated internal regulatory system for REE movement within the rice plant.

Notably, the geochemical signature of the grains, specifically the recovery of the Ce anomaly (δCe), was decoupled from bulk soil properties ($|r| < 0.22$). This lack of significant correlation reinforces the finding that the attenuation of the Ce anomaly is not a direct reflection of bulk soil geochemistry but is instead driven by localized processes at the soil-root interface or within the plant tissues.

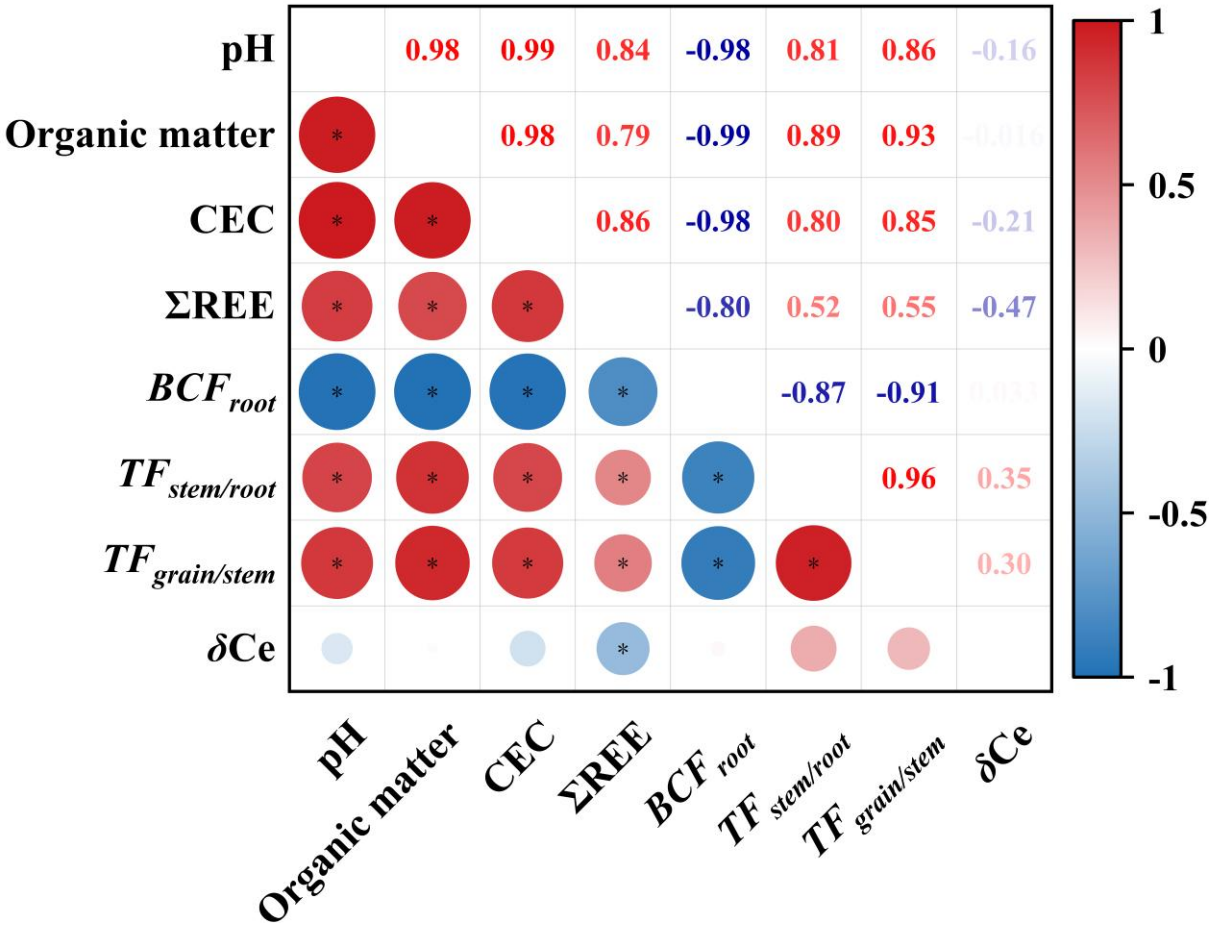


Fig. 5 Pearson correlation matrix between soil physicochemical properties and REE transfer parameters.

Note: The color scale indicates Pearson correlation coefficients (r); red and blue scales represent positive and negative Pearson correlation coefficients (r), respectively. REE, BCF, and TF represent rare earth element, bio-concentration factor, and translocation factor, respectively. CEC = cation exchange capacity; ∑REE = total REE concentration in soil; δCe = cerium anomaly in rice grain. Asterisks (*) denote statistical significance at the $p < 0.05$ level.

4 Discussion

4.1 Geogenic Inheritance and Geochemical Signaling of REEs in Karst Soils

The close similarity between the NASC-normalized REE patterns of karst soils and the underlying Middle Triassic Gejiu Formation limestones (Fig. 2) indicates a strong genetic link between the soil and its parent material. The pronounced negative Ce anomaly (δCe=0.76) observed in the karst soils serves as a diagnostic geochemical fingerprint inherited from marine carbonate rocks (Oladimeji et al. 2025; Yu et al. 2026). In oxidizing marine paleoenvironments, soluble Ce^{3+} is oxidized to the highly insoluble Ce^{4+} state, which is subsequently sequestered by manganese and iron oxyhydroxides or precipitated as cerianite, leading to a characteristic Ce depletion in the remaining seawater and the resulting carbonate sediments (Cao et al. 2025; Manceau et al. 2026). The preservation of this pronounced negative Ce anomaly during the transition from bedrock to residual soil indicates that the REE pool in the Qiubei karst area is predominantly geogenic. These results suggest minimal REE contributions from exogenous sources, such as atmospheric dust deposition or anthropogenic inputs (e.g., phosphate fertilizers), which typically exhibit flat or enriched Ce signatures (Li et al. 2025a; Oliveira et al. 2026).

Similarly, the moderate negative Eu anomaly (δEu = 0.65) in the karst soils is a signature inherited from the parent limestone, reflecting the composition of the upper continental crustal materials from which the carbonate precursors were derived (Wu et al. 2026; Zhang and Zhang 2026). During the intense chemical weathering of the Gejiu Formation limestones, the preferential leaching of mobile alkaline earth metals (Ca^{2+} and Mg^{2+}) leads to the residual accumulation of relatively immobile REEs in the terra rossa (Feng 2010; Yalçın et al. 2026). The consistency of these results with observations from other karst terrains in Guizhou and Guangxi (Cao et al. 2016; Dong et al. 2025) confirms that the weathering of Triassic carbonate successions imprints a remarkably stable and predictable REE geochemical signature on the agricultural soils of southwestern China. This geogenic high-background status provides a unique natural laboratory for investigating the long-term behavior of REEs in the soil-plant system.

4.2 Bioavailability and Physiological Barriers in the Soil-Rice System

The reduction in ∑REE concentrations from roots to grains by a factor of approximately 40 demonstrates the efficacy of physiological barriers in restricting REE translocation. The extremely low BCF_{root} (0.0045) suggests that the majority of REEs in the rhizosphere are either immobilized by soil minerals or sequestered within the root apoplast. Previous studies have indicated that REE ions, which possess high charge densities, are readily adsorbed onto the negatively charged sites of pectin in root cell walls (Guo et al. 2023; Zheng et al. 2023). The primary physiological bottleneck is the root endodermis, where the hydrophobic Casparian strip effectively blocks the apoplastic flow, forcing REEs to enter the symplastic route through selective plasma membrane transporters (Xu et al. 2003; Mohsin et al. 2026). Since REEs are non-essential elements with no specific transporters, their entry into the

vascular system is likely a low-affinity process, potentially occurring via calcium channels due to the similar ionic radii of REE^{3+} and Ca^{2+} (Alsherif et al. 2024; Liu et al. 2026a).

The secondary barrier is evident during the translocation from vegetative tissues to reproductive organs, as reflected by the low $TF_{grain/stem}$ value (0.110). This suggests that the phloem-mediated transport to developing grains is highly selective, effectively excluding REEs while prioritizing essential nutrients. Such a sequestration mechanism is biologically advantageous, as it prevents high concentrations of REEs from interfering with calcium-dependent signaling pathways and enzyme activities in the grain (Gjata et al. 2024; Martina et al. 2025).

The progressive decrease in the *LREE/HREE* ratio from roots (7.92) to grains (4.56) and the increasing trend of element-specific BCF_{root} values (Fig. 4) provide clear evidence of HREE-preferential mobility. This fractionation is primarily driven by the "lanthanide contraction," where HREEs, possessing smaller ionic radii, exhibit a higher affinity for forming stable, soluble complexes with organic ligands such as citrate and malate in the xylem and phloem sap (Grosjean et al. 2024). These soluble complexes are more mobile than the free $LREE^{3+}$ ions, which are more prone to adsorption or precipitation along the transport pathway (Wiche and Pourret 2023; Wu et al. 2025b).

Beyond physiological structures, the Pearson correlation analysis (Fig. 5) provides quantitative evidence that soil physicochemical properties act as the primary geochemical controls on REE bioavailability and internal translocation. The robust negative correlation between soil pH and BCF_{root} ($r = -0.983$) underscores that the near-neutrality of karst soils is a critical factor in limiting REE bioavailability. Under these conditions, REE ions are prone to precipitation as carbonates or hydroxides, and their adsorption onto Fe–Mn oxyhydroxides is significantly enhanced, thereby minimizing the pool of free REE^{3+} available for root interception (Ribeiro et al. 2024; Manceau et al. 2026).

The strong positive correlation between organic matter and $TF_{grain/stem}$ ($r = 0.927$) suggests a dual role for soil organic components. While organic matter contributes to the immobilization of REEs in the soil matrix (as evidenced by its negative correlation with BCF_{root}), the fraction of REEs that successfully enters the symplastic pathway may be complexed by low-molecular-weight organic ligands. These stable, soluble organic-REE complexes are more efficiently loaded into the phloem and translocated to the developing grains (Arciszewska et al. 2022). This dual-control mechanism—where pH restricts entry and organic ligands modulate internal transport—further explains why rice grains remain safe despite the high geogenic background of the soil. The integrated geochemical and physiological mechanisms governing REE behavior in the karst soil-rice system are conceptualized in Fig. 6.

The gradual "recovery" of the Ce anomaly (δCe increasing from 0.76 in soil to 0.89 in grain) is a particularly intriguing observation. In the oxidizing conditions of karst soils, a significant portion of Ce exists as immobile Ce^{4+} associated with Fe–Mn oxides, contributing to the strong negative anomaly inherited from the bedrock. However, in the reducing microenvironment of the rice rhizosphere, a fraction of Ce^{4+} may be reduced back to the more bioavailable Ce^{3+} (Giuliano et al. 2026). Consequently, the rice plant "samples" a REE pool that is less Ce-depleted than the bulk soil. Furthermore, the plant's

internal transport mechanisms may exhibit a slight kinetic preference for Ce^{3+} over its lanthanide neighbors, further attenuating the negative anomaly as REEs move toward the grain (Arbalestrie et al. 2022; Zhang and Shields 2022).

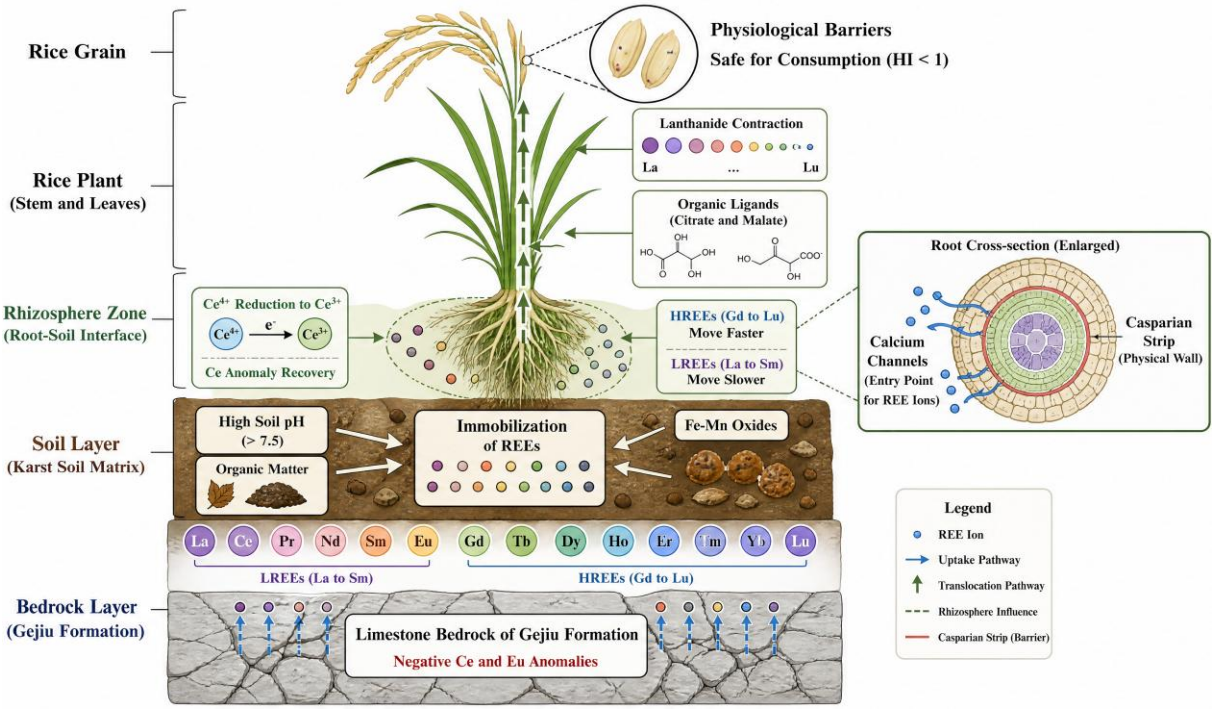


Fig. 6 Conceptual Model of Geochemical Behavior and Physiological Barriers of Rare Earth Elements (REEs) in the Soil–Rice System.

Note: The diagram summarizes the multi-stage mechanisms of REE fractionation and translocation in the karst catchment. (1) Geogenic Inheritance: The 14 REEs (La, Ce, Pr, Nd, Sm, Eu, Gd, Tb, Dy, Ho, Er, Tm, Yb, and Lu) originate from the Gejiu Formation limestone, inheriting negative Ce and Eu anomalies. (2) Geochemical Immobilization: Near-neutral soil pH and high organic matter content promote the adsorption and precipitation of REEs, limiting their bioavailability. (3) Rhizosphere Processes: Reducing conditions facilitate the reduction of Ce^{4+} to Ce^{3+}, leading to the recovery of the Ce anomaly. (4) Physiological Barriers: The Casparian strip and selective phloem loading act as critical bottlenecks, while REEs potentially enter via calcium channels. (5) Internal Fractionation: Driven by the lanthanide contraction, HREEs form stable complexes with organic ligands (e.g., citrate and malate), exhibiting higher mobility than LREEs. The synergy of these processes ensures the safety of rice grains for human consumption.

4.3 Implications for Food Safety and Regional Management

The findings of this study provide critical evidence that geogenic REE enrichment in karst soils does not necessarily translate into elevated health risks via the food chain. Despite the ∑REE in Qiubei karst soils (287.6 $mg \cdot kg^{-1}$) being significantly higher than the provincial background, the cumulative Hazard Index (HI) for local residents was only 0.158. This value is nearly an order of magnitude below the safety threshold of 1.0, indicating that the non-carcinogenic risk from rice consumption is negligible

(Astolfi et al. 2025; Hamza et al. 2026). This "high background, low risk" phenomenon is consistent with observations from other major karst regions in southwestern China, including Guizhou and Guangxi. As shown in our regional comparison, while soil REE levels vary across the karst belt due to different weathering intensities, the grain REE concentrations and associated HI values remain remarkably low and stable (Beckford et al. 2021; Luo et al. 2023; Zou et al. 2025). This regional coherence suggests that the physiological barrier mechanisms identified in Section 4.2 are a universal feature of rice plants adapted to karst geochemical environments.

These results have significant implications for public health policy and agricultural management in Yunnan's karst counties. Many of these regions are economically underdeveloped, and local communities often harbor concerns regarding "invisible contamination" from geogenic trace elements. Our quantitative risk assessment provides scientific reassurance that staple crops produced on limestone-derived soils are safe for consumption regarding REEs. Such evidence can be utilized by agricultural extension services to alleviate unwarranted public anxiety and support the development of "karst-origin" agricultural brands, emphasizing the safety and unique geochemical terroir of the region (Abebe et al. 2024; Ahmad et al. 2026).

However, it is essential to maintain a balanced perspective on food safety in karst terrains. While REEs appear to be effectively sequestered by plant barriers, other potentially toxic elements (PTEs), such as cadmium (Cd) and arsenic (As), are often geogenically enriched in carbonate-derived soils and may exhibit higher bioavailability than REEs (Liu et al. 2026c; Liu et al. 2026b). Therefore, future monitoring programs should adopt a multi-element approach to ensure comprehensive food safety. Furthermore, while the current HI suggests safety for adults, further research is needed to evaluate the long-term cumulative effects of REE exposure on more vulnerable populations, such as children and the elderly, particularly in areas where multiple exposure pathways (e.g., drinking water and dust inhalation) may coexist (Ye et al. 2025; Wu et al. 2025a).

5 Conclusions

This study elucidates the geochemical distribution, translocation mechanisms, and human health risks of REEs within a typical karst soil-rice system in Yunnan Province. Our findings demonstrate that the elevated REE concentrations in karst paddy soils are primarily a product of geogenic inheritance from the underlying Triassic Gejiu Formation, as evidenced by the preservation of diagnostic negative Ce and Eu anomalies. Despite this geogenic high-background status, the rice plant exhibits a remarkable capacity to exclude REEs, with concentrations decreasing by two orders of magnitude from the roots to the grains. This sharp acropetal reduction is governed by robust physiological barriers and is further modulated by soil-specific geochemical controls; notably, soil pH was identified as the primary determinant of REE bioavailability ($r = -0.983$), while organic matter plays a dual role in soil immobilization and internal translocation. Furthermore, a distinct internal fractionation was observed,

characterized by preferential HREE transport and a progressive attenuation of the negative Ce anomaly along the soil-root-grain pathway, likely driven by rhizosphere redox shifts and selective Ce^{3+} uptake. The cumulative hazard index of 0.158 confirms that rice consumption in this region poses negligible non-carcinogenic risks, supporting the "high geogenic background, low health risk" characteristic of karst carbonate terrains. Future research should integrate isotopic tracing and multi-element monitoring (e.g., Cd and As) to provide a more comprehensive assessment of food safety in these unique geochemical environments.

Acknowledgements We acknowledge the technical support from the Yunnan Soil Fertilizer and Pollution Repair Engineering Research Center and the research support from the Instrument Platform of the College of Resources and Environment, Huazhong Agricultural University.

Authors' contributions N.Z. contributed to the study conceptualization. Q.L. developed the methodology, performed the formal analysis, curated the data, and handled the software. Investigation, data validation, and visualization were conducted by Q.L., S.W., T.H., J.Z., X.S., and L.B. W.Z. and N.Z. provided resources, acquired funding, administered the project, and supervised the research. Q.L. wrote the original draft of the manuscript, and Q.L., W.Z., and N.Z. reviewed and edited the text. All authors reviewed the manuscript.

Funding This research was funded by the Innovation Guidance and Technology-based Enterprise Cultivation Program of Yunnan Provincial Science and Technology Department (Grant No. 202404BI090011) and the Fundamental Research Funds for the Central Universities of China (2662023DKPY003).

Data availability Data will be made available on request.

Declarations

Ethics approval Not applicable.
Consent to participate Not applicable.
Consent for publication Not applicable.
Conflict of interest The authors declare no competing interests.

References

Aarab I, Bounouira H, Amsil H, Maazouzi Y, Didi A, Badague A, Chakir EM (2026) Elemental composition and health risk assessment of heavy metals in medicinal plant Origanum elongatum from Northern Morocco. J Food Compos Anal 151:108945. https://doi.org/10.1016/j.jfca.2026.108945

Abebe Y, Alemayehu T, Birhanu B, Alamirew T, Alemayehu E (2024) Demystifying Heavy Metals and Physicochemical Characteristics of Groundwater in a Volcano-Tectonic Region of Middle Awash, Ethiopia, for Multipurpose Use. Sustainability 16(12):5257. https://doi.org/10.3390/su16125257

Ahmad T, Usman M, Almeetani M, Ahmed A, Qadir A, Hakeem MK, Shah I, Iltaf KH (2026) Heavy Metal(loid) Contamination in Groundwater of the Eastern Salt Range, Pakistan: Source Apportionment and Ecological-Human Health Risk Assessment. Earth Syst Environ. https://doi.org/10.1007/s41748-026-01187-3

Ain SNU, Abbasi AM, Ajab H, Faridullah, Khan S, Yaqub A (2023) Assessment of arsenic in Mangifera Indica (Mango) contaminated by artificial ripening agent: Target hazard quotient (THQ), health risk index (HRI) and estimated daily intake (EDI). Food Chem Adv 3:100468. https://doi.org/10.1016/j.focha.2023.100468

Alsherif EA, Sonbol H, AbdElgawad H, Ramadan A, Korany SM, Crecchio C, Ulhassan Z, Skalicky M, Yang X, Brestic M, Sheteiwy MS, Chen J, Bouqellah NA (2024) Arbuscular mycorrhizal fungi improve tolerance of wheat plants under soil Europium contamination. Plant Soil 505(1–2):881–895. https://doi.org/10.1007/s11104-024-06936-9

Arbalestrie B, Falys J, Bemelmans N, Thami A, Monin L, Devos E, Agnan Y (2022) Rare earth elements in an intercropping cover crop to evaluate the trace element transfer from soil to plant. Biogeochemistry 161(3):373–387. https://doi.org/10.1007/s10533-022-00989-7

Arciszewska Ż, Gama S, Leśniewska B, Malejko J, Nalewajko-Sieliwoniuk E, Zambrzycka-Szelewa E, Godlewska-Żyłkiewicz B (2022) The translocation pathways of rare earth elements from the environment to the food chain and their impact on human health. Process Saf Environ Prot 168:205–223. https://doi.org/10.1016/j.psep.2022.09.056

Astolfi ML, Jasan RC, Invernizzi R, Di Genaro C, Parrino F, Rapa M, Preti R, Conti ME (2025) Bromine and selected rare earth elements in Italian herbal teas by INAA: Exposure assessment. J Food Compos Anal 148:108448. https://doi.org/10.1016/j.jfca.2025.108448

Barrat J-A, Bayon G, Lalonde S (2023) Calculation of cerium and lanthanum anomalies in geological and environmental samples. Chem Geol 615:121202. https://doi.org/10.1016/j.chemgeo.2022.121202

Beckford HO, Chu H, Song C, Chang C, Ji H (2021) Geochemical characteristics and behaviour of elements during weathering and pedogenesis over karst area in Yunnan–Guizhou Plateau, southwestern China. Environ Earth Sci 80(2):61. https://doi.org/10.1007/s12665-020-09343-2

Cai Y, Xiao J, Liao X, Dong Y, Pan B, Zhang L, Xie G, Chen Y, Xie Y (2025) Dryland-to-Paddy Conversions Lead to Short-Term Decreases in Soil Organic Carbon and Carbon Pool Management Index in Karst Soil of Guizhou Province, China. Agriculture 15(4):396. https://doi.org/10.3390/agriculture15040396

Cao X, Wu P, Cao Z (2016) Element geochemical characteristics of a soil profile developed on dolostone in central Guizhou, southern China: implications for parent materials. Acta Geochim 35(4):445–462. https://doi.org/10.1007/s11631-016-0116-4

Cao Z, Zhang K, He J, Yang Z, Zhou Z (2021) Linking rocky desertification to soil erosion by investigating changes in soil magnetic susceptibility profiles on karst slopes. Geoderma 389:114949. https://doi.org/10.1016/j.geoderma.2021.114949

Cao M, Wei G, Zhang F, Ren X, Shi X, Lin Y, Li T, Chen S, Ling H, Cao J (2025) Molybdenum isotope

fractionations between ferromanganese oxides and seawater influenced ancient sedimentary isotopic signatures. Commun Earth Environ 6(1):565. https://doi.org/10.1038/s43247-025-02571-z

China National Environmental Monitoring Centre (1990) Background Values of Soil Elements in China. China Environmental Science Press, Beijing

Dong C, Han Z, Lu H, Zhao R, Cai Y, Li Y, Xu C, Zhang B (2024) Concentration, speciation, and fractionation of rare earth elements in alluvial soils in contiguous karst landform, southwestern China. J Geochem Explor 256:107360. https://doi.org/10.1016/j.gexplo.2023.107360

Dong C, Han Z, Wei X, Liu J, Zhao H, Gu Z, Zhang B, Xu C (2025) Occurrence and provenance of ion-adsorbed rare earth elements mineralization in alumina-rich rocks of the Permian Heshan formation, Western Guangxi, China. Appl Geochem 190:106498. https://doi.org/10.1016/j.apgeochem.2025.106498

Feng J (2010) Behaviour of rare earth elements and yttrium in ferromanganese concretions, gibbsite spots, and the surrounding terra rossa over dolomite during chemical weathering. Chem Geol 271(3–4):112–132. https://doi.org/10.1016/j.chemgeo.2010.01.003

Giuliano F, Tangredi DN, Guarino F, Castiglione S, Cicatelli A (2026) Effects of Gd^{3+} and Ce^{3+} on seed germination and growth of tomato and quinoa plants. Plant Biosyst 160(3):148. https://doi.org/10.1007/s44473-026-00154-0

Gjata I, Van Drimmelen CKE, Tommasi F, Paciolla C, Heise S (2024) Impact of Rare Earth Elements in sediments on the growth and photosynthetic efficiency of the benthic plant Myriophyllum aquaticum. J Soils Sediments 24(12):3814–3823. https://doi.org/10.1007/s11368-024-03867-x

Gromet LP, Haskin LA, Korotev RL, Dymek RF (1984) The “North American shale composite”: Its compilation, major and trace element characteristics. Geochim Cosmochim Acta 48(12):2469–2482. https://doi.org/10.1016/0016-7037(84)90298-9

Grosjean N, Blaudez D, Chalot M, Flayac J, Gross EM, Le Jean M (2024) Rare earth elements perturb root architecture and ion homeostasis in Arabidopsis thaliana. J Hazard Mater 468:133701. https://doi.org/10.1016/j.jhazmat.2024.133701

Guo Y, Chen K, Lei S, Gao Y, Yan S, Yuan M (2023) Rare Earth Elements (REEs) Adsorption and Detoxification Mechanisms in Cell Wall Polysaccharides of Phytolacca americana L. Plants 12(10):1981. https://doi.org/10.3390/plants12101981

Gutiérrez F, Parise M, De Waele J, Jourde H (2014) A review on natural and human-induced geohazards and impacts in karst. Earth-Sci Rev 138:61–88. https://doi.org/10.1016/j.earscirev.2014.08.002

Hamza A, Zhong L, Nawab J, Laghari Y, Ghani J, Khan S, Cui J, Wei Z (2026) Spatial Distribution, Health Risk Assessment and Source Apportionment of Potentially Toxic Elements in Soils Near Rare Earth Mining Areas of China: A Meta-Analysis. Bull Environ Contam Toxicol 116(1):17. https://doi.org/10.1007/s00128-025-04161-3

Han R, Xu Z (2021) Geochemical Behaviors of Rare Earth Elements (REEs) in Karst Soils under Different Land-Use Types: A Case in Yinjiang Karst Catchment, Southwest China. Int J Environ Res Public Health 18(2):502. https://doi.org/10.3390/ijerph18020502

Hao X, Hao H, Bu C, Long E, Wang H, Wu P, Li X (2026) Temporal and spatial distribution, sources and health risk assessment of trace elements in a typical karst river basin in Southwest China: Influence of acid mine drainage from abandoned coal mines. Ecotoxicol Environ Saf 309:119524.

https://doi.org/10.1016/j.ecoenv.2025.119524
Hartmann A, Goldscheider N, Wagener T, Lange J, Weiler M (2014) Karst water resources in a changing world: Review of hydrological modeling approaches: KARST WATER RESOURCES PREDICTION. Rev Geophys 52(3):218–242. https://doi.org/10.1002/2013RG000443
Jiang Z, Lian Y, Qin X (2014) Rocky desertification in Southwest China: Impacts, causes, and restoration. Earth-Sci Rev 132:1–12. https://doi.org/10.1016/j.earscirev.2014.01.005
Laveuf C, Cornu S (2009) A review on the potentiality of Rare Earth Elements to trace pedogenetic processes. Geoderma 154(1–2):1–12. https://doi.org/10.1016/j.geoderma.2009.10.002
Li G, Meng Y, Zhou J, Ming D, Dai L, Wang L (2025a) Geochemical characteristics and source analysis of rare earth elements in Qinghai Lake sediments. Acta Geochim 44(2):231–246. https://doi.org/10.1007/s11631-025-00763-0
Li X, Xie M, Yang K, Li K, Han C, She H, Liang G, Li X, Fan H (2025b) Calcium-O-Sr-Nd isotope evidence for the origin of REE-bearing carbonatite from metasomatized lithospheric mantle without recycled carbonate. Contrib Mineral Petrol 180(8):46. https://doi.org/10.1007/s00410-025-02239-z
Liu K, Guan X, Li G, Duan M, Li Y, Hong Y, Lin M, Fu R, Yu F (2022) Publication characteristics, topic trends and knowledge domains of karst ecological restoration: a bibliometric and knowledge mapping analysis from 1991 to 2021. Plant Soil 475(1–2):169–189. https://doi.org/10.1007/s11104-022-05345-0
Liu J, Li H, Wang R, Xu J, Saputro SP, Godang S (2025) Weathering and REE enriching processes in the Nanxiong deposit, South China: Insights from whole-rock and multi-mineral geochronology and geochemistry. Ore Geol Rev 186:106936. https://doi.org/10.1016/j.oregeorev.2025.106936
Liu C, Zhao J, Liu W, Van Der Ent A, Qiu R, Morel JL, Tang Y (2026a) The effect of rare earth elements (REEs) on plant growth promotion: a review on mechanisms and the role of REE-dependent methylotrophs. Plant Soil 518(1):959–974. https://doi.org/10.1007/s11104-025-08041-x
Liu Z, Sun G, Wu X, Yu W, Yao H, Lin Y, Fu C, Liu J, Feng X (2026b) Analysis of cadmium sources in surface soil in typical karst regions: Anthropogenic input contribution and atmospheric transport impact. J Hazard Mater 504:141349. https://doi.org/10.1016/j.jhazmat.2026.141349
Liu Z, Zeng Y, Wang W, Zhang B, Liu J, Zhao X (2026c) Coupling positive matrix factorization with machine learning to quantify contamination sources and map health risks of heavy metals in karst soils. Soil Environ Health 4(1):100193. https://doi.org/10.1016/j.seh.2026.100193
Luo C, Liang P, Yang R, Gao J, Chen Q, Mo H (2023) Mineralogical and Geochemical Constraints on the Occurrence Forms of REEs in Carboniferous Karst Bauxite, Central Guizhou Province, Southwest China: A Case Study of Lindai Bauxite. Minerals 13(3):320. https://doi.org/10.3390/min13030320
Manceau A, Liao J, Li Y, Giacomelli A, Retegan M, Koschinsky A, Steinmann SN, Mathon O (2026) Oxidative uptake of Ce by oceanic ferromanganese crusts and implications for paleoredox estimates using Ce isotopes. Commun Earth Environ 7(1):172. https://doi.org/10.1038/s43247-026-03196-6
Martina A, Ferroni L, Marrocchino E (2025) The Soil–Plant Continuity of Rare Earth Elements: Insights into an Enigmatic Class of Xenobiotics and Their Interactions with Plant Structures and Processes. J Xenobiotics 15(2):46. https://doi.org/10.3390/jox15020046
Mohsin M, Ramzan M, Baltrėnaitė-Gedienė E, Nawrot N, Kaipiainen E, Rasheed F, Zafar Z, Wojciechowska E, Pappinen A, Kuittinen S (2026) Growth and Phytostabilization Potential of Willow under Rare Earth

Elements Exposure in Floating Treatment Wetlands. Water Air Soil Pollut 237(3):124. https://doi.org/10.1007/s11270-025-08829-8

Mori C, Dellwig O, Wollschläger J, Seidel M (2025) Process zone specific alteration of rare earth element (REE) patterns across the land–ocean transition of the southern North Sea. Geochim Cosmochim Acta 402:32–48. https://doi.org/10.1016/j.gca.2025.06.017

Oladimeji RG, Idakwo SO, Adeleye MA, Musa A (2025) Possible sources of REE, Paleo-redox conditions, and diagenetic history of Paleocene limestone from Ewekoro formation, Eastern Dahomey Basin, Southwestern Nigeria. Discov Geosci 3(1):74. https://doi.org/10.1007/s44288-025-00179-6

Oliveira ES, Garnier J, Araújo DF, Mulholland DS, Dias-Roque DF, Tonha MS, Cicerelli RE, Koide S, Bonnet MP, Seyler P, Roig HL (2026) Sources, mobility, and accumulation of major and trace elements in sediments: implications for environmental quality and management of an urbanized tropical lake (Brasília, Brazil). Limnology 27(2):277–292. https://doi.org/10.1007/s10201-025-00823-7

Pagano G, Guida M, Tommasi F, Oral R (2015) Health effects and toxicity mechanisms of rare earth elements—Knowledge gaps and research prospects. Ecotoxicol Environ Saf 115:40–48. https://doi.org/10.1016/j.ecoenv.2015.01.030

Ribeiro PG, De Oliveira C, Guerra MBB, De Carvalho TS, Martins GC, Pereira WVDS, Ramos SJ, Guilherme LRG (2024) Rare Earths as Emerging Trace Element Contaminants in the Soil. Curr Pollut Rep 10(3):443–458. https://doi.org/10.1007/s40726-024-00312-y

Shi P, Zhang T, Liu Z, Lan J, Fan X (2019) A Vulnerable Environment Study in Karst Regions between 1991 and 2017: A Bibliometric Analysis. Appl Sci 9(24):5339. https://doi.org/10.3390/app9245339

Shi N, Zhu J, Liu X, Zhang S, Meng G, Zhang H, Cheng J, Zhou J, Lu B, Dao J, Mi X, Fan M (2025) Geochemistry and U–Pb geochronology of the granite porphyry in Bainiuchang, Southeastern Yunnan, China. Acta Geochim 44(2):325–347. https://doi.org/10.1007/s11631-024-00750-x

Sun K, Deng J, Wang Q, Chen B, Xu R, Ma Z (2023) Formation of Sn-rich granitic magma: a case study of the highly evolved Kafang granite in the Gejiu tin polymetallic ore district, South China. Miner Deposita 58(2):359–378. https://doi.org/10.1007/s00126-022-01130-2

U.S. Environmental Protection Agency (1989) IRIS toxicological review of cadmium. Integrated Risk Information System. https://iris.epa.gov/ChemicalLanding/&substance_nmbr=141. Accessed 1 May 2026

Veress M (2020) Karst Types and Their Karstification. J Earth Sci 31(3):621–634. https://doi.org/10.1007/s12583-020-1306-x

Wang W, Yang Y, Wang D, Huang L (2024) Toxic Effects of Rare Earth Elements on Human Health: A Review. Toxics 12(5):317. https://doi.org/10.3390/toxics12050317

Wang S, Yao Y, Wang J, Ruan B, Yu Y (2025) Advancing Stress-Resilient Rice: Mechanisms, Genes, and Breeding Strategies. Agriculture 15(7):721. https://doi.org/10.3390/agriculture15070721

Wiche O, Pourret O (2023) The role of root carboxylate release on rare earth element (hyper)accumulation in plants – a biogeochemical perspective on rhizosphere chemistry. Plant Soil 492(1–2):79–90. https://doi.org/10.1007/s11104-023-06177-2

Wu Y, Hui Y, Zhang L, Li J, Wu Y, Liu X, Liu X (2025a) Rare Earth Element Exposure and Gestational Diabetes Mellitus: Insights into the Coexistence of Environmental Exposure Risks and Benefits. Expo Health 17(4):905–919. https://doi.org/10.1007/s12403-025-00701-8

Wu Z, Liu J, Li C, Liu W, Wu W (2025b) Redistribution and enhanced bioavailability of rare earth elements speciation induced by mining-driven transformation in ionic rare earth mining areas. Sci Rep 15(1):27345. https://doi.org/10.1038/s41598-025-13513-2

Wu J, Li X, Liu F, An Y, Wang W, Ling M, Zhang Z (2026) The Ce isotopic composition of the upper continental crust constraints from loess and granites. Solid Earth Sci 11(2):100303. https://doi.org/10.1016/j.sesci.2026.100303

Xiong G, Yu W, Du Y, Weng S, Pang D, Deng X, Zhou J (2021) Provenance of Lower Carboniferous Bauxite Deposits in Northern Guizhou, China: Constraints from Geochemistry and Detrital Zircon U-Pb Ages. J Earth Sci 32(1):235–252. https://doi.org/10.1007/s12583-020-1081-8

Xu X, Zhu W, Wang Z, Witkamp G-J (2003) Accumulation of rare earth elements in maize plants (*Zea mays* L.) after application of mixtures of rare earth elements and lanthanum. Plant Soil 252(2):267–277. https://doi.org/10.1023/A:1024715523670

Xu X, Yan Y, Dai Q, Gan F, Ghoneim SSM (2025a) Tracing soil erosion processes in Karst regions using rare earth elements: The role of bedrock outcrops and seasonal impacts. Int Soil Water Conserv Res 13(3):675–686. https://doi.org/10.1016/j.iswcr.2025.04.001

Xu Y, Li Y, Wang P, Feng C, Cao S, Li J (2025b) Unraveling the geochemical behaviors of rare earth elements (REEs) in Chinese drinking natural mineral waters: Environmental and health perspectives. J Hazard Mater 494:138731. https://doi.org/10.1016/j.jhazmat.2025.138731

Xu L, Li X, Tang L, Yang F, Shi Z, Cheng B, Liu X, Cheng X (2026) Synergistic Inhibition Effect of Cd in Soil–Rice System from a Ca and Zn Enriched Karst Paddy: A Field-Based Study. Agriculture 16(5):501. https://doi.org/10.3390/agriculture16050501

Yalçın C, Kochan P, Uras Y (2026) Geochemical and Statistical Analysis of Terra Rossa Clay Minerals: a Case Study from Osmaniye Almanpinari Region, Türkiye. Lithol Miner Resour 61(1):94–113. https://doi.org/10.1134/S0024490225700312

Yang D, Sui H, Mao W, Wang Y, Yang D, Zhang L, Liu Z, Yong L, Song Y (2022) Dietary Exposure Assessment of Rare Earth Elements in the Chinese Population. Int J Environ Res Public Health 19(23):15583. https://doi.org/10.3390/ijerph192315583

Ye S, Zhang R, Wu P, Zhao D, Chen J, Pan X, Wang J, Zhang H, Qi X, Weng Q, Lu Z, Zhou B (2025) Occurrence and Exposure Assessment of Rare Earth Elements in Zhejiang Province, China. Foods 14(11):1963. https://doi.org/10.3390/foods14111963

Yu H, Zhang H, Zhang X, Jiang J, Liang Y, Chen L, Zeng G (2026) Characteristics and Potential Origin of Carbonate Components in the Louisville Seamounts. J Earth Sci 37(1):36–49. https://doi.org/10.1007/s12583-024-0027-y

Yun J, Yang Q, Zhao C, Chen C, Liu G (2024) Atmospheric emissions of fine particle matter bound rare earth elements from industry. Nat Commun 15(1):9338. https://doi.org/10.1038/s41467-024-53684-6

Zaghum MJ, Ali K, Teng S (2022) Integrated Genetic and Omics Approaches for the Regulation of Nutritional Activities in Rice (*Oryza sativa* L.). Agriculture 12(11):1757. https://doi.org/10.3390/agriculture12111757

Zhang D, Shen X, Ruan Q, Xu X, Yang S, Lu Y, Xu H, Hao F (2014) Effects of subchronic samarium exposure on the histopathological structure and apoptosis regulation in mouse testis. Environ Toxicol Pharmacol

37(2):505–512. https://doi.org/10.1016/j.etap.2014.01.007

Zhang Q, Han G, Liu M, Wang L (2019) Geochemical Characteristics of Rare Earth Elements in Soils from Puding Karst Critical Zone Observatory, Southwest China. Sustainability 11(18):4963. https://doi.org/10.3390/su11184963

Zhang K, Shields GA (2022) Sedimentary Ce anomalies: Secular change and implications for paleoenvironmental evolution. Earth-Sci Rev 229:104015. https://doi.org/10.1016/j.earscirev.2022.104015

Zhang H, Zhang H (2026) Pyroxenite Xenoliths Reveal the Comprehensive Existence of Subduction-Related Mantle Metasomatism in Continental Lithosphere beneath the Northwestern North China Craton. J Earth Sci. https://doi.org/10.1007/s12583-026-2047-2

Zheng H, Yang Y, Liu W, Zhong Y, Cao Y, Qiu R, Liu C, Van Der Ent A, Hodson MJ, Tang Y (2023) Rare earth elements detoxification mechanism in the hyperaccumulator Dicranopteris linearis: [silicon-pectin] matrix fixation. J Hazard Mater 452:131254. https://doi.org/10.1016/j.jhazmat.2023.131254

Zou Z, Zhang S, Yuan J, Ying X, Tao Z, Luo S (2025) Sustainable Exploration, Mining, and Utilization of a Rare Earth Deposit in Southeastern Guangxi: Insights into Metallogenic Regularity. Sustainability 17(6):2552. https://doi.org/10.3390/su17062552

Supplementary Files

This is a list of supplementary files associated with this preprint. Click to download.

- GraphicalAbstract.png